



## Effect of Surface Roughness on Brinell Hardness and Load-Displacement Curves using a Macro Indentation

A. Karbasian, M. Shirazi, A. H. Mahmoudi\*

*Mechanical Engineering Department, Bu-Ali Sina University, Hamedan, Iran*

### PAPER INFO

#### Paper history:

Received 06 February 2023

Received in revised form 03 March 2023

Accepted 04 March 2023

#### Keywords:

Macro Spherical Indentation

Roughness

Brinell Hardness

Load-displacement Curve

Finite Element Simulation

### ABSTRACT

Surface roughness significantly affects the scattering of load-displacement curves and the measurement of mechanical properties by the macro-scale indentation. Many mechanical properties such as modulus of elasticity, yield stress, strain hardening exponent, and hardness can be determined using the indentation results, which are the information obtained from the load-displacement curve. Reliable parameters of the load-displacement (P-h) curve are employed to estimate the mechanical properties. The inaccurate P-h curve leads to a misestimation of material properties. Ignoring the surface roughness might be a source of error in the indentation results. In this paper, the effects of surface roughness on the P-h curve of macro spherical indentation and Brinell hardness number (BHN) were studied. The range of roughness with minimal effect on indentation results was obtained. The surface roughness of 2 and 12 microns was created on the experimental samples using the electrical discharge machining (EDM) process. The finite element simulations were performed with different surface roughnesses. The results showed that roughness affected both the P-h curve and hardness values in different indentation depths and various indenter sizes. It was observed that with increasing the Rq roughness, the P-h curve level and hardness value decreased and that with increasing the indentation depth, the effect of roughness on hardness decreased as well. The numerical results showed a good agreement with the results of experiments.

doi: 10.5829/ije.2023.36.05b.08

## 1. INTRODUCTION

The determination of material properties in engineering material has always been a subject of concern. Employing the indentation method is one of the non-destructive and effective methods to estimate the material properties; therefore, unreliable and inaccurate data of the indentation result is usually a source of error. Surface roughness is one of the important parameters which may cause uncertainties in indentation results, when is neglected. The indentation technique relies on the characterization of the P-h curve parameters. In general, surface roughness is determined using the peaks and valleys of the surface and their interval distribution along the surface [1]. In the indentation method, surface roughness can play an important role in the determination of mechanical properties. Studies showed that surface roughness can alter the P-h curves [2, 3]. However, it

should be noted that most of the studies have been carried out on the nano and micro scales. Surface roughness in the low-depth indentations can be one of the primary sources of error in estimation of various mechanical properties. In the large indentation depth, the error at the contact point is reduced. It has been revealed that the error caused by the surface roughness is proportional to the indentation depth [4]. Surface roughness is effective when the dimensions of peaks and valleys are much smaller than dimension of the contact area [5]. Since the contact area of the indenter and the surface can be obtained indirectly from the indentation depth, surface roughness can cause errors in determination of the contact area between the indenter and the surface piece [1]. Bhaskara Rao and Beatrice Seventlin [6] developed a new technique based on the image processing to measure the surface roughness.

\*Corresponding Author Email: [a.h.mahmoudi@gmail.com](mailto:a.h.mahmoudi@gmail.com),  
[a.h.mahmoudi@basu.ac.ir](mailto:a.h.mahmoudi@basu.ac.ir) (A. H. Mahmoudi)

Walter et al. [7] assessed the effect of surface roughness on elastic modulus using 2D and 3D FEM simulation on a Nano scale. They realized that for  $Ra > 3$  nm, the results varied considerably in both models. Campbell et al. [8] investigated the effect of roughness on the reduced modulus ( $E_r$ ) in impact of two surfaces and presented a principle study using three-dimensional finite element modeling to implement the apparent modulus in a rough surface, which was measured by an atomic force microscope (AFM). Chen et al. [9] reported that when the applied forces are small, the surface roughness has a significant effect (due to the low level of indentation). However, this issue is not of importance in case of sharp indenters. They also developed a 3D roughness model using a Berkovich indenter in ABAQUS software. Gao et al. [10] studied the effect of surface roughness on variables such as indentation force, contact area, and contact load in both loading and unloading. They modeled the roughness of different materials by mapping the experimental AFM data to a finite element model. Xia et al. [11] presented various quantitative models for estimating macro-hardness in studying the effect of roughness on hardness. The effect of non-reproducibility as an error of the Nano-indentation test was taken into consideration. Bobji et al. [12] studied the effect of roughness on a macro scale with an average point height of 1 mm for different roughness shapes with a spherical indenter. They found that Young's modulus and hardness are sensitive to roughness. Furthermore, they studied the quasi-static indentation to determine the results of scatter due to the surface roughness parameters. Bobji et al. [13] found that the hardness scatterings measured on a rough surface in Nano-indentation could be caused by geometric change of roughness during indentation, the effect of indenter geometry, and the material properties. In another case, they suggested that the hardness value is reliable when the indentation depth "h" is greater than or equal to four times the value of the Root Mean Square (RMS or  $R_q$ ) of the profile height parameter. Tang et al. [14] studied the influence of surface roughness on hardness measurement by using nano indentation tests and FE analysis. Xia [15] advised a method to accurately determine the mechanical properties, taking into account the calculation of the errors in the first contact point and also the effect of the surface roughness error. Using 2D Finite Element (FE) analysis of spherical indentation on a Nano scale, Walter et al. [16] observed that increasing the roughness decreased the contact area and, as a result, there was more scattering of the Young's modulus in an elastic deformation. They also stated that when the roughness value is much smaller than the contact surface, the geometric parameter of roughness has a significant effect on the results of the indentation process. In another case, they found that increasing the roughness led to more scattering of the P-h curve. Nazemian et al. [17] showed

that the surface roughness of thin films affects the Nanoindentation results, especially at low indentation depth. Mikowski et al. [18] determined the mechanical properties of the kaolinite material considering the effect of surface roughness in the Nano-indentation test on their samples. Bolesta and Fomin [19] found that the surface around the indentation area changed due to the surface roughness. In some cases, the accuracy of measuring the hardness and the P-h curve can be affected by these changes. Maslenikov et al. [20] resulted that the roughness deviates the hardness from its correct number. They corrected the hardness value by information of correlation function and height distribution. Jiang et al. [21] examined the effect of surface roughness on the nano hardness and elastic modulus of thin films. They used nano-indentation method to extract the material properties. They also showed that the micro hardness and elastic modulus decreased in rough samples in comparison with smooth ones.

Pham et al. [22] proposed a function from FE and regression analysis by using spherical indentation to determine the plastic properties of materials. Goto et al. [23] obtained the stress - strain curve by employing an estimation technique based on the indentation method. Wagih [24] employed a sharp nano-indentation test and FE analysis to predict the hardness of composite and pure metal. Akahori et al. [25] also used the spherical indentation and numerical method to measure the yield stress and residual stresses.

In recent years, the indentation method, numerical inverse analysis, and FE simulations have been widely used to determine the material properties of various materials [26-28]. Bocciarelli and Maier [29] employed the imprint area and indentation test to estimate the residual stresses. Furthermore, studies have been performed for simultaneous determination of the material model and the residual stresses for different materials [30, 31].

As it was previously mentioned, many of the methods which have been proposed to estimate the material properties from the indentation approach, are based on the P-h curve parameters. Access to an accurate P-h curve is one of the complex challenges. An inaccurate P-h curve can lead to incorrect and scattered material properties. Different surface roughnesses can alter the P-h curves. It is one of the challenges to recognize the effect of roughness on the P-h curve and roughness range that does not affect the curves.

In this paper, the effect of surface roughness on the hardness value and P-h curve of the macro-spherical indentation was studied. The effects of the indenter size and the indentation depth were examined and compared for different rough surfaces. Most of the previous studies have been conducted for nano scale indentation and roughness. Finite Element Analysis with different surface roughness were performed to specify the effects

of roughness, indenter size, and indentation depth on both P-h curves and the Brinell hardness. The optimum roughness range within which the effect of micro roughness on the macro P-h curves results could be ignored, was obtained. The Finite Element (FE) results were also verified using several experimental tests.

**2. RESEARCH METHOD**

The procedure of this research is described in the flowchart as shown in Figure 1.

**2. 1. Roughness Simulation** In this study, one of the challenges was modeling of the surface roughness. Despite many efforts, it was noticed that 3D modeling of the surface roughness in ABAQUS commercial code was complicated. For this purpose, a rough surface was first modeled in MATLAB coding commercial software and N×N points were created using a random statistical function. Then, by mapping the points from MATLAB to ABAQUS, the desired model with a specified Rq was modeled in ABAQUS [32-34].

The parameter Rq represents the distribution of the standard deviation in the surface point’s height, which is an essential parameter for creating the surface roughness by statistical methods. This parameter represents the root mean square (RMS) of the profile height from the mean line and is more sensitive to the parameter Ra (arithmetic mean of the height of the points) in deviations of large surfaces from the mean line. Rq or RMS is defined by Equation (1) [35]:

$$R_q = \sqrt{\frac{1}{L} \int_0^L [Z(x)]^2 dx} \tag{1}$$

where in Equation (1), L is the sampling length and Z is the height of the points from the origin of the coordinate system .

The following smart and novel method was employed to model the rough surface. First, a rough surface with the desired Rq was created on the N×N point in MATLAB coding program. Then, all steps of the indentation simulation were performed in ABAQUS. The resulted rough surface was then mapped from the MATLAB to the indentation area in ABAQUS using the JAVA coding program. Figure 2 shows the created rough surface in MATLAB and Figure 3 illustrates the mapped surfaces to the FE model for different roughness values.

**2. 2. Finite Element Method** Finite element simulations were performed using ABAQUS commercial code. The indenter was modelled with a Young’s modulus of 600 GPa, and a Poisson’s ratio of 0.3 [36], which corresponds to the properties of tungsten carbide. The elastic regime was considered for the indenter material. Due to the symmetry in loading and geometry,

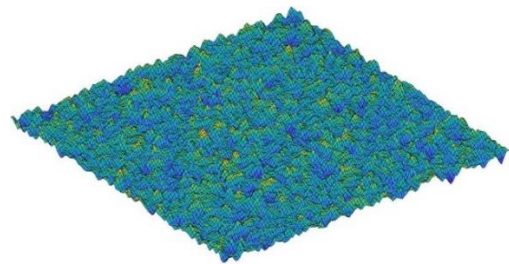


**Figure 2.** 3D rough surface schematic obtained from MATLAB software

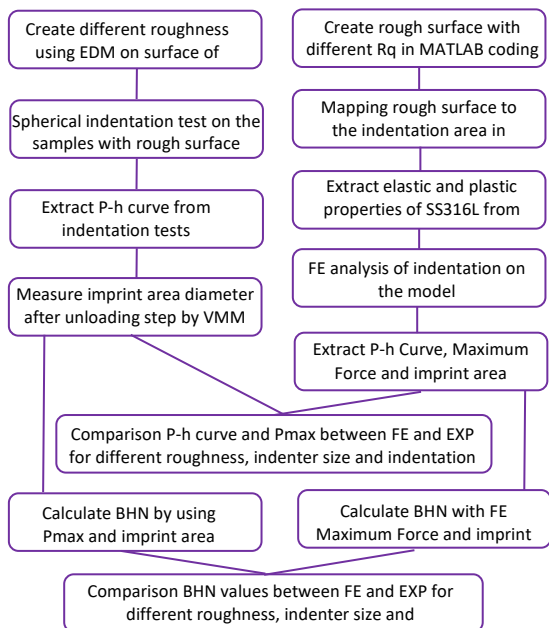


**Figure 1.** A Schematic presentation of the research flow diagram

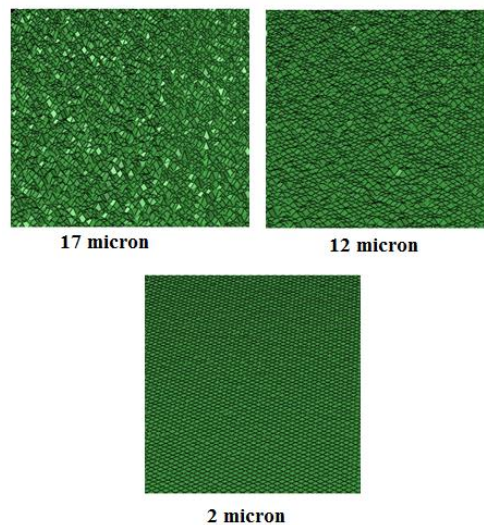


**Figure 3.** Roughness schematic created in ABAQUS

only a quarter of the sample was modelled for both the indenter and the specimen. The materials regime for the sample was considered to be elastic-plastic with a Young's modulus of 204 GPa, which was extracted from the uniaxial tensile test of stainless steel 316L, and the Poisson's ratio was considered to be 0.3 [37]. The plastic true strain-stress data extracted from the tensile test was used as the plastic properties. The type of the element used in the spherical indenter and specimen was C3D8R. The mesh size was 0.03 mm which was verified by a convergence checking. Figure 4 shows the P-h curve convergence. The total number of elements were 336,000. Spherical indenters with diameters of 1, 1.5, 2.5, and 4 mm and a block with dimensions of 3×4×4 mm<sup>3</sup> were modelled. Figure 5 illustrates the imprint area and deformation of the sample in the Y direction after the unloading step.

**2. 3. Hardness Calculation Method** The Brinell method is a two-stage indentation procedure to determine the hardness. In the first step, a hard indenter is pressed vertically into the surface of the sample under load. In the second step, the length of the indentation diameters is measured from at least two perpendicular directions. Equation (2) shows the Brinell's hardness equation [38, 39]. The Brinell hardness value is obtained by dividing the applied force by the area of the indented surface.

$$BHN = 0.102 \times \frac{2F}{\pi D(D - \sqrt{D^2 - d^2})} \tag{2}$$

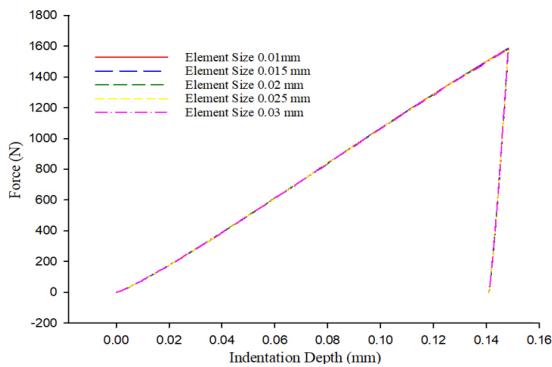


Figure 4. Convergence for the P-h curves

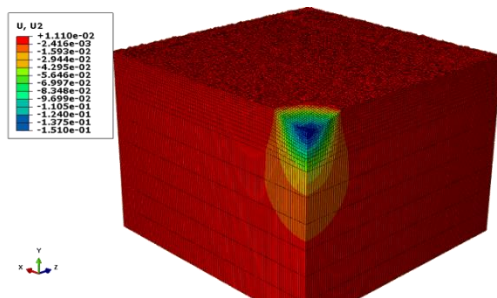


Figure 5. Deformed view of the FE model after unloading

In the above equation, BHN is the Brinell hardness value in (kg/mm<sup>2</sup>), F is the force, D and d represent the diameter of the indenter and the diameter of the indentation imprint in (mm), respectively. In calculation of the hardness, the values of the force and the indentation imprint diameter were extracted from both numerical and experimental imprints. The force used in the hardness calculation was the maximum contact force (P<sub>max</sub>) between the specimen and indenter. The P<sub>max</sub> was extracted from the end of loading step of the P-h curve.

**2. 4. Experimental Tests** The material used in this study was stainless steel 316L. This grade of steel is widely used in marine structures, food devices, medical implants, and fasteners [40]. The samples for tensile tests were manufactured according to standard ASTM E 8M-04 [41]. In Figure 6 the true and engineering stress-strain curves of 316L are shown. The yield stress and elastic modulus of the specimen were 263Mpa and 204GPa, respectively. Furthermore, the chemical compositions of 316L are appicted in Table 1.

The indentation tests were carried out using a universal tension-compression test device with a capacity of 5000 N. The indentation depth was measured by a linear variable differential transformer (LVDT) with accuracy of 0.1 micron. In Figure 7 the indentation test setup and its components are shown. Both load and indentation depth were recorded during the indentation tests.

An electric discharge machine (EDM) was used to create the required roughness on the block samples manufactured from stainless steel 316L. The EDM affects the morphology and roughness parameters of the material's surface [42]. The 2- and 12-micron roughness

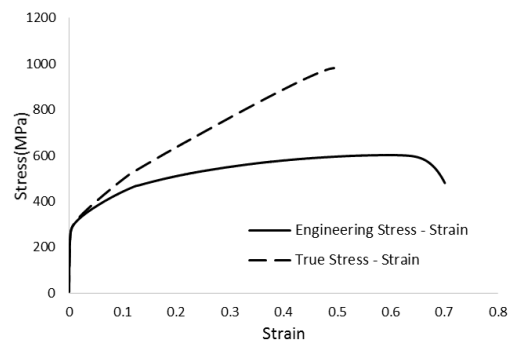


Figure 6. True and engineering stress - strain curves of 316L

TABLE 1. Chemical composition of experimented SS316L

Fe	C	Si	Mn	P	S	Cr	Mo
Base	0.024	0.41	1.79	0.020	0.013	16.95	2.034
Ni	Al	Co	Cu	Nb	Ti	V	W
10.06	0.004	0.41	0.41	0.008	0.002	0.053	0.077



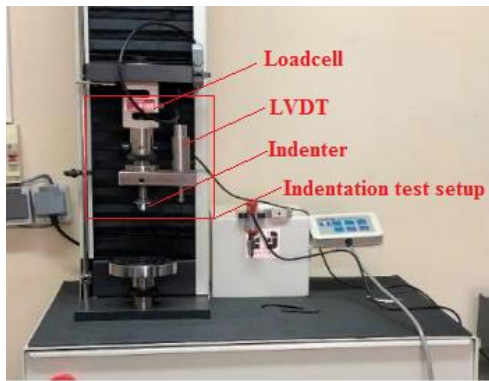


Figure 7. Macro spherical indentation test setup

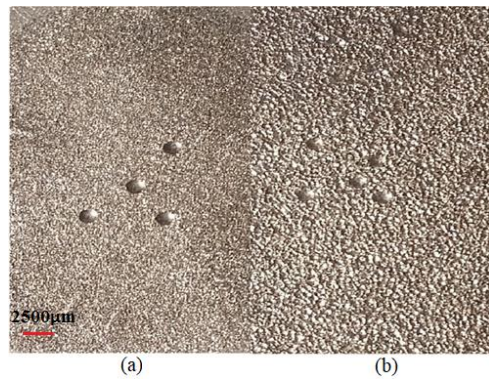


Figure 8. Two surfaces with different  $R_q$  roughness values (a) 2-microns (b) 12-microns

were achieved by changing the EDM input parameters, such as current intensity and the pulse time. Figure 8 shows two surfaces with different roughness values along with the imprints of the indentation remained after unloading. The advantage of having more diverse roughness values was provided by the application of the EDM to create the roughness. Although there are other techniques to create the roughness, the EDM process provided the requirement surface roughness with the least side effects.

Two indenters with diameters of 2.5 and 1.5 mm were employed in the experimental indentation test; therefore, the effect of the indenter size and the roughness could be observed simultaneously. Also, the indentation depths of 50, 90, and 150 microns were examined on the samples to investigate the effect of indentation depth of the rough surface on the spherical indentation. The diameters of the indentation imprint were measured using a vision measuring machine (VMM) in four different directions with high accuracy. The measurements were performed along different directions to achieve more accurate results. Then, the Brinell hardness was calculated using Equation (2). A surface profilometer was used to measure the roughness. Three important roughness parameters were obtained according to Table 2.  $R_a$  is the arithmetic mean of profile height,  $R_p$  is the maximum profile peak, and  $R_v$  is the maximum profile valley depth. In Table 2, the standard deviation (SD) of measured parameters are shown.

### 3. RESULTS AND DISCUSSION

#### 3. 1. Effect of Roughness on Load Displacement Curve

Several finite element analyses with the  $R_q$  roughness values of 2, 7, 12, and 17-micron were performed. Figure 9 compares the P-h curves obtained from numerical simulations and experimental tests for 2 and 12-micron roughness using a 2.5-mm diameter indenter. The P-h curves for the 1.5-mm indenter with 2-

TABLE 2. Roughness parameters measured by surface profilometry device, (SD: Standard deviation)

Roughness ( $R_q$ )	$R_a$ , $\mu\text{m}$ (SD)	$R_p$ , $\mu\text{m}$ (SD)	$R_v$ , $\mu\text{m}$ (SD)
2-micron	1.56 (0.16)	4.66 (0.33)	5.1 (0.36)
12-micron	9.6 (0.59)	36.5 (4.84)	34 (3.45)

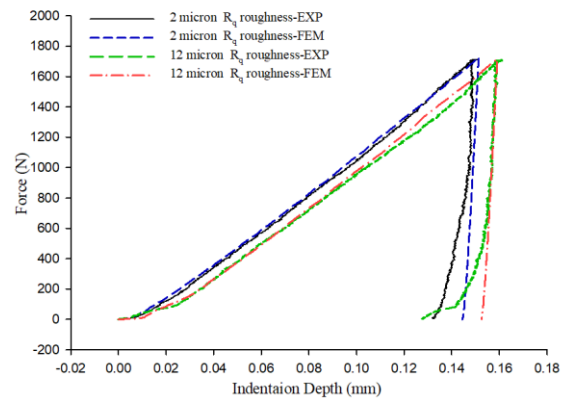
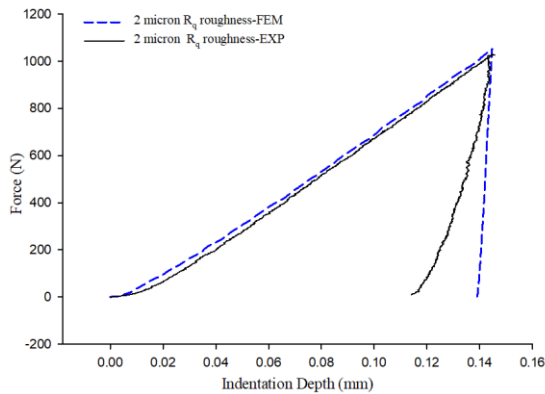


Figure 9. Comparison of P-h curves related to the 2.5 mm indenter in both 2 and 12-micron  $R_q$  roughness between FE results and experimental tests

micron roughness are shown in Figure 10 According to these figures, the P-h curves obtained from the finite element simulations illustrated a good agreement with the results from the experimental tests. In all figures the FEM, EXP and Dia are the abbreviations of finite element results, experimental results and diameter of indenter.

It is observed in Figure 9 that with the decrease in the surface roughness, the P-h curves were elevated in both the numerical and experimental results. This is mainly due to the less amount of load required for indentation in the case of 12-micron roughness. This is especially more observable in the beginning of the curves due to less



**Figure 10.** P-h curves, 1.5mm diameter indenter, 2-micron Rq roughness: A comparison between FE and experiments

materials constraint of a rough surface. The curve slopes were also less at the beginning for the case of 12-micron roughness .

The experiment tests revealed that by increasing the surface roughness, the scattering of the P-h curves was increased. Little difference between the P-h curves relates to different points of surface for each roughness value was observed, but there was a meaningful difference between the indentation test results of various roughness.

Although the unloading step of the P-h curve was not the subject of this study, according to Figures 9 and 10, a considerable difference with FE was observed. This deviation was related to the indentation unloading test setup. However, no parameter has been extracted for this study from the unloading section of the curves and therefore this deviation did not affect the results. The loading part of the curves displayed a good agreement between the numerical and experimental results. Similar deviation was observed in other research [43].

In order to further clarify the effect of roughness on the P-h curves 7 and 17 micron roughness were also modeled. Figure 11 shows a comparison between their P-h curves and the 2 and 12-micron cases. Curves in Figure 11 also confirmed the above discussion.

**3. 2. Effect of Indenter Diameter**

The diameters of the spherical indenters were selected in such a way that significant differences were observed in the results. Figures 12 and 13 illustrate the effects of 1, 1.5, 2.5, and 4 mm diameter indenters on the numerically obtained P-h curves resulting from the indentation on surfaces with 2 and 12 micron roughness. Trends of the curves were the same in both 2 and 12 micron roughness and the P-h curves were elevated with an increase in the indenter size. Table 3 shows the maximum force at 150-micron indentation depth for different conditions. The maximum deviation between forces of 2 and 12-micron roughness

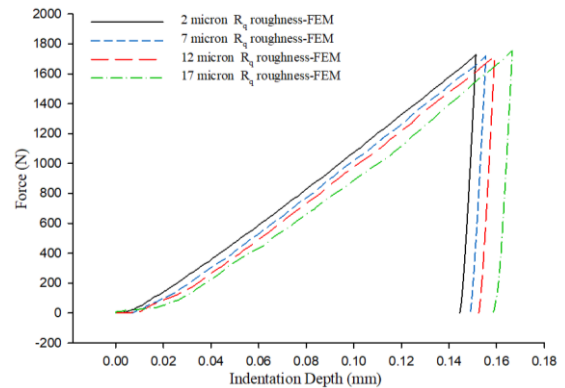


**Figure 11.** Effect of Rq roughness on the FE P-h curves

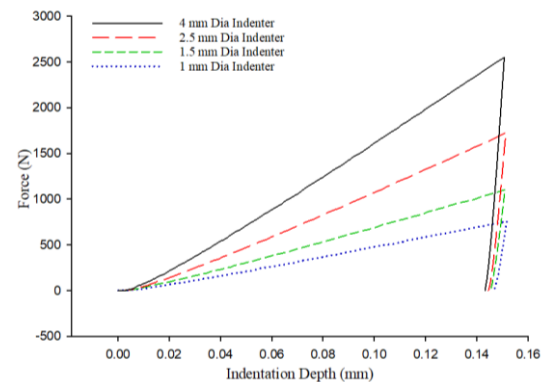


**Figure 12.** Comparison between FE P-h curves for different indenter sizes and 2-micron surface roughness

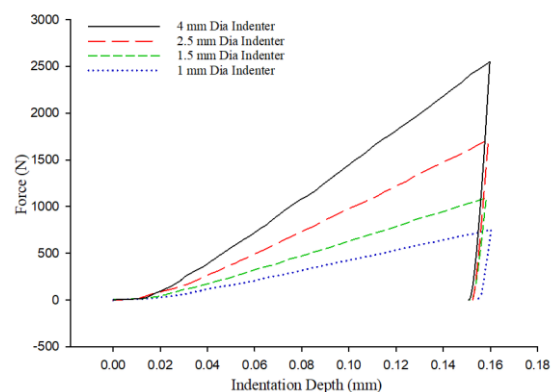


**Figure 13.** Comparison between FE P-h curves for different indenter sizes and 12-micron Rq roughness

was for the 1mm diameter indenter with a value of 7.07% and the minimum was related to the 4-mm-diameter indenter with a value of 6.18%. According to the presented results of Figures 12 and 13 and Table 3, it was concluded that the spherical indentations with larger indenter sizes were less affected by the surface

roughness. In the comparison of the experimental P-h curves between the 1.5 and 2.5mm indenters, a great reduction in the force of 1.5-mm-diameter indenter was observed (Figure 14).

**3. 3. Optimum Roughness Range** It was observed that the roughness of 2 micron and less was an appropriate range within which the effect of roughness on the P-h curves resulting from the 2.5-mm-diameter spherical indentation could be ignored. As shown in Figures 15 and 16, the P-h curves of 2-micron Rq roughness and the ideal surface (without roughness in the numerical model and polished surface in the experiment) indicated a good agreement. There are slight differences between the 3-micron roughness and the two other curves in the numerical results shown in Figure 15.

The deviation of 2 and 3-micron roughness P-h curves was related to the early loading stage of curves where the peaks and valleys of the surface have the maximum effect on the indentation force. It can be noted that a 2-micron roughness surface and less are a reliable range for spherical macro indentation.

**TABLE 3.** Maximum force values at the indentation depth of 150-microns caused by 1, 1.5, 2.5 and 4 mm diameter indenter in FE simulations

Indenter diameter (mm)	Rq Roughness (micron)	Force (N)	Deviation between forces (%)
1	2	748.7	7.07
	12	695.8	
1.5	2	1099	6.73
	12	1025	
2.5	2	1708.9	6.62
	12	1595.7	
4	2	2536.9	6.18
	12	2380.2	

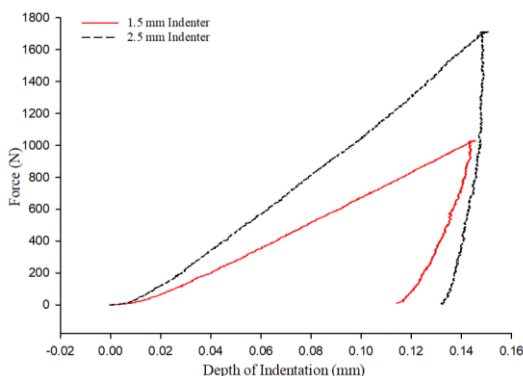


**Figure 14.** Comparison between experimental P-h curves with 1.5 and 2.5 mm indenter

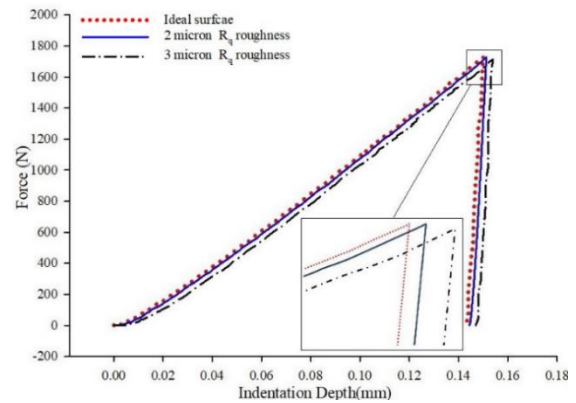


**Figure 15.** Comparison of the FE P-h curves between the 2- and 3-micron roughness and the ideal surface for the 2.5-mm indenter

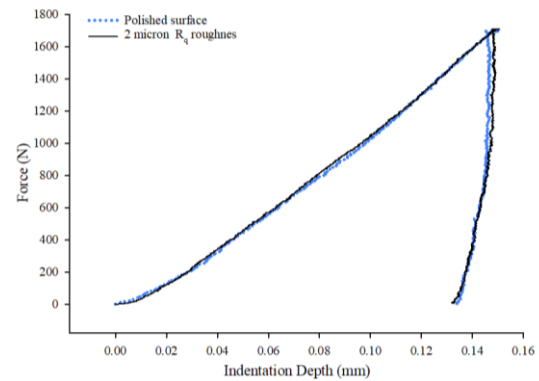


**Figure 16.** Comparison of the EXP P-h curves between the 2-micron Rq roughness and the polished surface for the 2.5-mm indenter

**3. 4. Effect of Roughness on Hardness** Figure 17 shows the Brinell hardness with a diameter of 2.5 mm for 2 and 12-micron roughness at 150, 90, and 50-micron indentation depths. The hardness values increased with a decrease in roughness for both numerical and experimental results. The slope of curves in the measured hardness based on the FE data was lower than the experimental hardness, indicating that the FE hardness values of 2 and 12 microns Rq roughness are closer to each other than the experimental values. The hardness values at 90 and 150-micron indentation depths were convergent, suggesting that the 50-micron indentation depth was not an appropriate depth considering the roughness values.

Indentation tests were performed at a depth of 150 microns with a 1.5-mm indenter on the 2 and 12-micron roughness to investigate the effect of the indenter size on the measured hardness. The FE simulations were also carried out using the same diameter and indentation depth and the corresponding hardness values were determined as shown in Figure 18. The trend of changes in the

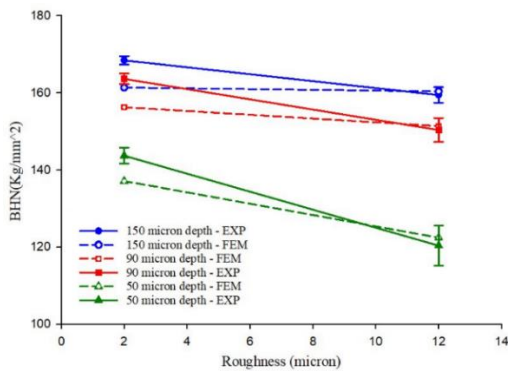


**Figure 17.** Comparison of the hardness for 2- and 12-micron Rq roughness and different indentation depths for both the FE and experimental results

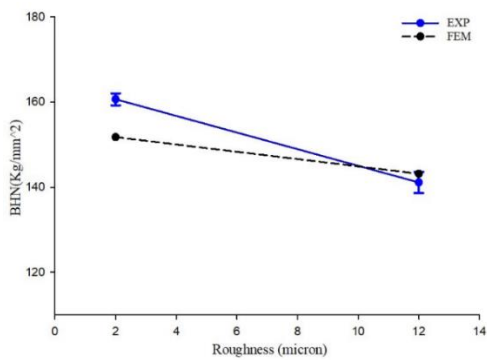


**Figure 18.** Effect of roughness on hardness values in FE and experimental results with the 1.5-mm-diameter indenter

**TABLE 4.** All hardness values with different indenter size, indentation depth and surface roughness

Indenter diameter (mm)	Indentation depth (µm)	FE/ EXP	Rq Roughness (µm)	BHN (kgf/mm <sup>2</sup> )
2.5	50	EXP	2	143.7
			12	120.4
	FE	2	137.1	
		12	122.4	
2.5	90	EXP	2	163.6
			12	150.3
	FE	2	156.3	
		12	151.4	
2.5	150	EXP	2	168.4
			12	159.3
	FE	2	161.4	
		12	160.3	
1.5	150	EXP	2	160.3
			12	141.1
	FE	2	151.8	
		12	143.2	

hardness with the 1.5-mm diameter indenter was the same as previous results shown in Figure 17. All calculated values of hardness are depicted in Table 4.

The influence of both the indentation depth and surface roughness on the measurement of hardness is shown in Figure 19. The figure contains the measured hardness values of both numerical and experimental results. It can be noted that the hardness values of the surface with 2 micron roughness were higher than the 12-micron roughness and this is mainly due to the higher values of force in the indentation with 2-micron roughness. The measured values of hardness became closer together with an increase in the indentation depth. Therefore, it can be concluded that with an increase in the indentation depth, the effect of roughness on the hardness decreased.

Based on the standard deviation values of Figures 17 and 19, it can be concluded by increasing the roughness, the BHN scattering increased. The reason based on Table 2, is the higher standard deviation of 12-micron roughness compared to 2-micron roughness. Figure 19 Shows that by increasing indentation depth, the hardness values deviations decreased in both 2 and 12-micron roughnesses. There are two reasons for this subject: first the difficulties and errors of measuring the imprint area in the low-depth indentation due to the presence of roughness and second the better repeatability of maximum force in deeper indentation.

Finally, the numerical results showing the effects of wider range of surface roughness on the hardness values are shown in Figure 20. In this figure the hardness values for different roughness of 2, 7, 12, and 17-microns with a 150-micron indentation depth were compared. The results also confirmed the previous discussion.

The results of this study had a good agreement with other research. Chen et al. [9] by employing sharp nano-indentation, concluded roughness in the nano scale affects the P-h curve and hardness. They resulted in that by decreasing the surface roughness from 20 nm to 2 nm

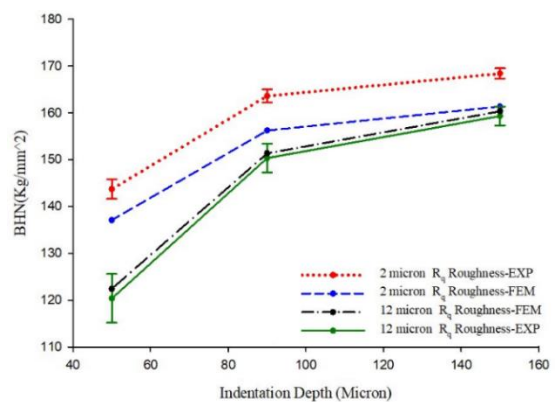


**Figure 19.** Comparison between the curves of experimental and numerical hardness for the 2.5-mm-indenter with 2- and 12-micron Rq roughness and indentation depths of 50, 90, and 150 microns



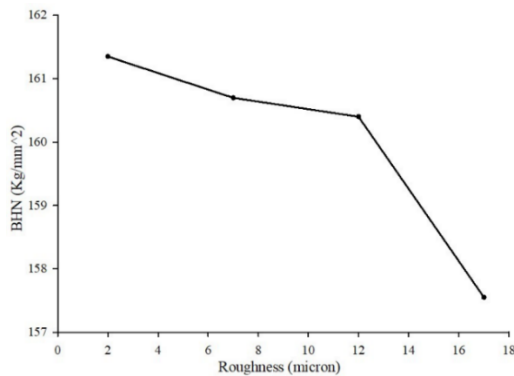


**Figure 20.** Comparison of hardness in 2, 7, 12, and 17-micron Rq roughness

in 362 nm indentation depth, the P-h curve elevated. The scattering of P-h curves and hardness numbers were minimum in 2 nm roughness. In the current study, similar results were obtained from macro spherical indentation on the rough surfaces.

#### 4. CONCLUSIONS

In this study, the effect of surface roughness on the P-h curves and hardness of macro spherical indentation was investigated. In this regard, a rough surface was modeled and several FE simulations and experimental tests with different surface roughness, indentation depths, and indenter sizes were performed. Findings of this work can be concisely expressed below:

- With decreasing the Rq roughness, the P-h curves elevated and the hardness values increased.
- With increasing the indenter diameter for indentation on the rough surfaces, the effect of Rq roughness on the P-h curves and hardness decreased .
- An increase in depth of indention played a significant role in decreasing the effect of Rq roughness in both the P-h curves and the hardness values. The values of hardness were closer with increasing the indentation depth for different values of roughness.
- The Rq roughness of 2 microns and less was a range within which the effect of roughness on the P-h curves for the 2.5-mm-diameter indenter and 150-micron indentation depth could be ignored.
- By increasing the roughness, the scattering in measured hardness increased.

#### 5. REFERENCES

1. Fischer-Cripps, A.C. and Nicholson, D., "Nanoindentation. Mechanical engineering series", *Applied Mechanics Reviews*, Vol. 57, No. 2, (2004), B12-B12.
2. Marteau, J., Jourani, A. and Bigerelle, M., "Determination of an objective criterion for the assessment of the feasibility of an instrumented indentation test on rough surfaces", *Materials*, Vol. 13, No. 7, (2020), 1589. <https://doi.org/10.3390/ma13071589>
3. Marteau, J. and Bigerelle, M., "Toward an understanding of the effect of surface roughness on instrumented indentation results", *Journal of Materials Science*, Vol. 52, (2017), 7239-7255. <https://doi.org/10.1007/s10853-017-0961-5>
4. Standardization, I.O.f., "Metallic materials: Instrumented indentation test for hardness and materials parameters. Test method, ISO, (2015).
5. Johnson, K.L. and Johnson, K.L., "Contact mechanics, Cambridge university press, (1987).
6. Bhaskara Rao, J. and Beatrice Seventline, J., "Estimation of roughness parameters of a surface using different image enhancement techniques", *International Journal of Engineering, Transactions B: Applications*, Vol. 30, No. 5, (2017), 652-658. doi: 10.5829/idosi.ije.2017.30.05b.04.
7. Walter, C. and Mitterer, C., "3d versus 2d finite element simulation of the effect of surface roughness on nanoindentation of hard coatings", *Surface and Coatings Technology*, Vol. 203, No. 20-21, (2009), 3286-3290. <https://doi.org/10.1016/j.surfcoat.2009.04.006>
8. Campbell, A.C., Buršiková, V., Martinek, J. and Klapetek, P., "Modeling the influence of roughness on nanoindentation data using finite element analysis", *International Journal of Mechanical Sciences*, Vol. 161, (2019), 105015. <https://doi.org/10.1016/j.ijmeosci.2019.105015>
9. Chen, L., Ahadi, A., Zhou, J. and Ståhl, J.-E., "Modeling effect of surface roughness on nanoindentation tests", *Procedia CIRP*, Vol. 8, (2013), 334-339. doi: 10.1016/j.procir.2013.06.112.
10. Gao, C., Proudhon, H. and Liu, M., "Three-dimensional finite element analysis of shallow indentation of rough strain-hardening surface", *Friction*, Vol. 7, (2019), 587-602. <https://doi.org/10.1007/s40544-018-0245-3>
11. Xia, Y., Bigerelle, M., Marteau, J., Mazeran, P.E., Bouvier, S. and Iost, A., "Effect of surface roughness in the determination of the mechanical properties of material using nanoindentation test", *Scanning: The Journal of Scanning Microscopies*, Vol. 36, No. 1, (2014), 134-149. doi: 10.1002/sca.21111.
12. Bobji, M., Shivakumar, K., Alehossein, H., Venkateshwarlu, V. and Biswas, S., "Influence of surface roughness on the scatter in hardness measurements—a numerical study", *International Journal of Rock Mechanics and Mining Sciences*, Vol. 36, No. 3, (1999), 399-404. [http://dx.doi.org/10.1016/S0148-9062\(99\)00009-1](http://dx.doi.org/10.1016/S0148-9062(99)00009-1)
13. Bobji, M. and Biswas, S., "Deconvolution of hardness from data obtained from nanoindentation of rough surfaces", *Journal of Materials Research*, Vol. 14, No. 6, (1999), 2259-2268. <https://doi.org/10.1557/JMR.1999.0302>
14. Tang, D., Zhao, L., Wang, H., Li, D., Peng, Y. and Wu, P., "The role of rough surface in the size-dependent behavior upon nano-indentation", *Mechanics of Materials*, Vol. 157, (2021), 103836. <https://doi.org/10.1016/j.mechmat.2021.103836>
15. Xia, Y., "A robust statistical method for determining material properties and indentation size effect using instrumented indentation testing", Université de Technologie de Compiègne, (2014),
16. Walter, C., Antretter, T., Daniel, R. and Mitterer, C., "Finite element simulation of the effect of surface roughness on nanoindentation of thin films with spherical indenters", *Surface and Coatings Technology*, Vol. 202, No. 4-7, (2007), 1103-1107. doi: 10.1016/j.surfcoat.2007.07.038.
17. Nazemian, M., Chamani, M. and Baghani, M., "A combined experimental and numerical study of the effect of surface roughness on nanoindentation", *International Journal of Applied Mechanics*, Vol. 11, No. 07, (2019), 1950070. <https://doi.org/10.1142/S1758825119500704>

18. Mikowski, A., Soares, P., Wypych, F., Gardolinski, J. and Lepienski, C., "Mechanical properties of kaolinite 'macro-crystals'", *Philosophical Magazine*, Vol. 87, No. 29, (2007), 4445-4459. doi: 10.1080/14786430701550394.
19. Bolesta, A. and Fomin, V., "Molecular dynamics simulation of sphere indentation in a thin copper film", *Physical Mesomechanics*, Vol. 12, No. 3-4, (2009), 117-123. <https://doi.org/10.1016/j.physme.2009.07.003>
20. Maslenikov, I., Useinov, A., Birykov, A. and Reshetov, V., "Reducing the influence of the surface roughness on the hardness measurement using instrumented indentation test", in IOP Conference Series: Materials Science and Engineering, IOP Publishing. Vol. 256, (2017), 012003.
21. Jiang, W.-G., Su, J.-J. and Feng, X.-Q., "Effect of surface roughness on nanoindentation test of thin films", *Engineering Fracture Mechanics*, Vol. 75, No. 17, (2008), 4965-4972. doi: 10.1016/j.engfracmech.2008.06.016.
22. Pham, T.-H., Phan, Q.-M. and Kim, S.-E., "Identification of the plastic properties of structural steel using spherical indentation", *Materials Science and Engineering: A*, Vol. 711, (2018), 44-61. <https://doi.org/10.1016/j.msea.2017.10.097>
23. Goto, K., Watanabe, I. and Ohmura, T., "Determining suitable parameters for inverse estimation of plastic properties based on indentation marks", *International Journal of Plasticity*, Vol. 116, (2019), 81-90. doi: 10.1016/j.ijplas.2018.12.007.
24. Wagih, A., "Experimental and finite element simulation of nano-indentation on metal matrix composites: Hardness prediction", *International Journal of Engineering, Transactions A: Basics*, Vol. 29, No. 1, (2016), 78-86. doi: 10.5829/idosi.ije.2016.29.01a.11.
25. Akahori, T., Nagakura, T., Fushimi, S. and Yonezu, A., "An indentation method for evaluating the residual stress of polymeric materials: Equi-biaxial and non-equi-biaxial residual stress states", *Polymer Testing*, Vol. 70, (2018), 378-388. doi: 10.1016/j.polymertesting.2018.07.024.
26. Hosseinzadeh, A. and Mahmoudi, A., "Determination of mechanical properties using sharp macro-indentation method and genetic algorithm", *Mechanics of Materials*, Vol. 114, (2017), 57-68. doi: 10.1016/j.mechmat.2017.07.004.
27. Xia, J., Won, C., Kim, H., Lee, W. and Yoon, J., "Artificial neural networks for predicting plastic anisotropy of sheet metals based on indentation test", *Materials*, Vol. 15, No. 5, (2022), 1714. <https://doi.org/10.3390/ma15051714>
28. Luo, C. and Yuan, H., "Determination of elastoplastic properties in anisotropic materials with cubic symmetry by instrumented indentation", *Mechanics of Materials*, Vol. 174, (2022), 104461. <https://doi.org/10.1016/j.mechmat.2022.104461>
29. Bocciairelli, M. and Maier, G., "Indentation and imprint mapping method for identification of residual stresses", *Computational Materials Science*, Vol. 39, No. 2, (2007), 381-392. <https://doi.org/10.1016/j.commatsci.2006.07.001>
30. Salmani Ghanbari, S. and Mahmoudi, A., "An improvement in data interpretation to estimate residual stresses and mechanical properties using instrumented indentation: A comparison between machine learning and kriging model", *Engineering Applications of Artificial Intelligence*, Vol. 114, (2022). <https://doi.org/10.1016/j.engappai.2022.105186>
31. Wang, Z., Deng, L. and Zhao, J., "A novel method to extract the equi-biaxial residual stress and mechanical properties of metal materials by continuous spherical indentation test", *Materials Research Express*, Vol. 6, No. 3, (2018), 036512. doi: 10.1088/2053-1591/aeca6.
32. Gascón, F. and Salazar, F., "Simulation of rough surfaces and analysis of roughness by matlab", *MATLAB—A Ubiquitous Tool for the Practical Engineer*, InTech, Rijeka, (2011), 391-420. doi: 10.5772/22534.
33. Wu, J.-J., "Simulation of rough surfaces with fft", *Tribology International*, Vol. 33, No. 1, (2000), 47-58. [http://dx.doi.org/10.1016/S0301-679X\(00\)00016-5](http://dx.doi.org/10.1016/S0301-679X(00)00016-5)
34. Garcia, N. and Stoll, E., "Monte carlo calculation for electromagnetic-wave scattering from random rough surfaces", *Physical Review Letters*, Vol. 52, No. 20, (1984), 1798. <https://doi.org/10.1103/PhysRevLett.52.1798>
35. Luo, Y., Wang, Y., Guo, H., Liu, X., Luo, Y. and Liu, Y., "Relationship between joint roughness coefficient and statistical roughness parameters and its sensitivity to sampling interval", *Sustainability*, Vol. 14, No. 20, (2022), 13597. <https://doi.org/10.3390/su142013597>
36. Mahmoudi, A., Ghanbari-Matloob, M. and Nourbakhsh, S., "A novel method to determine material properties and residual stresses simultaneously using spherical indentation", *Journal of Testing and Evaluation*, Vol. 43, (2015), 87-95. doi: 10.1520/JTE20130236.
37. Zhong, T., He, K., Li, H. and Yang, L., "Mechanical properties of lightweight 316l stainless steel lattice structures fabricated by selective laser melting", *Materials & Design*, Vol. 181, (2019), 108076. doi: 10.1016/j.matdes.2019.108076.
38. Kim, S.-H., Jeon, E.-c. and Kwon, D., "Determining brinell hardness from analysis of indentation load-depth curve without optical measurement", *Journal of Engineering Materials and Technology*, Vol. 127, No. 1, (2005), 154-158. <https://doi.org/10.1115/1.1839213>
39. International, A., "Standard test method for brinell hardness of metallic materials", ASTM International, (2012).
40. Jooya, M., Hosseinzadeh, A.R. and Mahmoudi, A., "Plasticity effect on residual stresses measurement using contour method", *International Journal of Engineering, Transactions A: Basics*, Vol. 26, No. 10, (2013), 1203-1212. doi: 10.5829/idosi.ije.2013.26.10a.10.
41. ASTM, E., "Standard test methods for tension testing of metallic materials", *Annual Book of ASTM Standards*. ASTM, Vol., No., (2001).
42. Phan, N., Dong, P., Muthuramalingam, T., Thien, N., Dung, H., Hung, T., Duc, N. and Ly, N., "Experimental investigation of uncoated electrode and pvd alcrni coating on surface roughness in electrical discharge machining of ti-6al-4v", *International Journal of Engineering, Transactions A: Basics*, Vol. 34, No. 4, (2021), 928-934. doi: 10.5829/ije.2021.34.04a.19.
43. Yonezu, A., Yoneda, K., Hirakata, H., Sakihara, M. and Minoshima, K., "A simple method to evaluate anisotropic plastic properties based on dimensionless function of single spherical indentation-application to sic whisker-reinforced aluminum alloy", *Materials Science and Engineering: A*, Vol. 527, No. 29-30, (2010), 7646-7657. doi: 10.1016/j.msea.2010.08.014.

## Persian Abstract

## چکیده

زبری سطح به طور قابل توجهی بر پراکندگی منحنی های بار-جابجایی و اندازه گیری خواص مکانیکی توسط نفوذ در مقیاس ماکرو تأثیر می گذارد. بسیاری از خواص مکانیکی مانند مدول الاستیسیته، تنش تسلیم، توان کرنش سختی و سختی را می توان با استفاده از نتایج نفوذ، که اطلاعات به دست آمده از منحنی بار-جابجایی است، تخمین زد. پارامترهای قابل اعتماد منحنی بار-جابجایی (P-h) برای تخمین خواص مکانیکی استفاده می شود. منحنی P-h غیر دقیق، منجر به تخمین نادرست خواص مواد می شود. نادیده گرفتن زبری سطح ممکن است یک منبع خطا در نتایج نفوذ باشد. در این مقاله، اثرات زبری سطح بر روی منحنی نیرو - عمق نفوذ و عدد سختی برینل (BHN) مورد بررسی قرار گرفت. محدوده زبری با کمترین تأثیر بر روی نتایج نفوذ کروی به دست آمد. زبری سطح ۲ و ۱۲ میکرون بر روی نمونه های آزمایشی با استفاده از فرآیند ماشینکاری تخلیه الکتریکی (EDM) ایجاد شد. شبیه سازی اجزای محدود با زبری های سطحی مختلف انجام شد. نتایج نشان داد که زبری بر منحنی P-h و مقادیر سختی در عمق نفوذ های مختلف با نفوذگرهای با سایزهای مختلف، تأثیر می گذارد. مشاهده شد که با افزایش زبری Rq، سطح منحنی P-h و مقدار سختی کاهش یافت و با افزایش عمق فرورفتگی، تأثیر زبری بر سختی نیز کاهش یافت. نتایج تطابق خوبی بین شبیه سازی FE و آزمون تجربی نشان داد.